

# On-X Heart Valve Prosthesis: Numerical Simulation of Hemodynamic Performance in Accelerating Systole

NIMA MIRKHANI,<sup>1</sup> MOHAMMAD REZA DAVOUDI,<sup>2</sup> PEDRAM HANAFIZADEH,<sup>1</sup> DARYOOSH JAVIDI,<sup>3</sup>  
and NILOOFAR SAFFARIAN<sup>4</sup>

<sup>1</sup>Center of Excellence in Design and Optimization of Energy Systems, School of Mechanical Engineering, College of Engineering, University of Tehran, Tehran, Iran; <sup>2</sup>Biomedical Engineering, Katholieke Universiteit Leuven, Louvain, Belgium; <sup>3</sup>Department of Cardiac Surgery, Pars Hospital, Tehran, Iran; and <sup>4</sup>Cardiovascular Department, Pars Hospital, Tehran, Iran

(Received 29 January 2016; accepted 26 April 2016; published online 10 May 2016)

Associate Editor Ajit P. Yoganathan oversaw the review of this article.

**Abstract**—Numerical simulation of the bileaflet mechanical heart valves (BMHVs) has been of interest for many researchers due to its capability of predicting hemodynamic performance. A lot of studies have tried to simulate this three-dimensional complex flow in order to analyze the effect of different valve designs on the blood flow pattern. However, simplified models and prescribed motion for the leaflets were utilized. In this paper, transient complex blood flow in the location of ascending aorta has been investigated in a realistic model by fully coupled simulation. Geometry model for the aorta and the replaced valve is constructed based on the medical images and extracted point clouds. A 23-mm On-X Medical BMHV as the new generation design has been selected for the flow field analysis. The two-way coupling simulation is conducted throughout the accelerating phase in order to obtain valve dynamics in the opening process. The complex flow field in the hinge recess is captured precisely for all leaflet positions and recirculating zones and elevated shear stress areas have been observed. Results indicate that On-X valve yields relatively less transvalvular pressure gradient which would lower cardiac external work. Furthermore, converging inlet leads to a more uniform flow and consequently less turbulent eddies. However, the leaflets cannot open fully due to middle diffuser-shaped orifice. In addition, asymmetric butterfly-shaped hinge design and converging orifice leads to better hemodynamic performance. With the help of two-way fluid solid interaction simulation, leaflet angle follows the experimental trends more precisely rather than the prescribed motion in previous 3D simulations.

**Keywords**—Fluid solid interaction, Hemodynamic performance, Bileaflet mechanical heart valve.

## INTRODUCTION

Surgical operation and replacement of the diseased native heart valves is a common procedure for the patients who suffer from heart valve disease. Mal-functioning valves are usually replaced by artificial heart valves, for which an increasing demand is seen each year. Considering the fact that about 55% of the diseased heart valves are substituted by artificial mechanical ones, this type of the prosthetic valves are recently the choice for many surgeons. It has been reported that about 80% of the implanted mechanical heart valves in the aortic position are bileaflet mechanical heart valves (BMHVs).<sup>20,43,45</sup> BMHVs are mainly constructed with artificial materials like pyrolytic carbon and therefore they show acceptable strength and durability, however patients with these implants require long-term anticoagulant therapy.<sup>12,13,41</sup> This phenomenon is attributed to the non-physiological blood flow pattern which is created by this artificial organ in the heart.<sup>21</sup>

On the other hand, Computational Fluid Dynamics (CFD) are among the powerful tools generally for the study of cardiovascular risk factors<sup>15</sup> and especially those related to the mechanical performance of the artificial valves.<sup>12,23,42</sup> In the case of BMHVs, the dynamic of the leaflets play an important role in the flow pattern through the valve and its motion is fully coupled with the physiologic blood flow. Therefore, here comes the turn to the Fluid Solid Interaction (FSI) simulation which accounts for this coupled physics associated with this problem.<sup>41</sup> This numerical simulation is capable of transfer data between the solid boundaries, i.e., valve leaflets, and the fluid domain which is blood flow in the ascending aorta for this case.

Address correspondence to Pedram Hanafizadeh, Center of Excellence in Design and Optimization of Energy Systems, School of Mechanical Engineering, College of Engineering, University of Tehran, Tehran, Iran. Electronic mail: hanafizadeh@ut.ac.ir

A lot of researchers tried to utilize different numerical methods in order to better understand the flow pattern in implanted valves especially BMHVs.

Earlier hemodynamic simulation of the BMHVs were almost limited to steady state and fixed leaflets assumptions. King *et al.*<sup>24–26</sup> has been done early researches about the hemodynamic performance of BMHVs in several works. They first conducted a 2D steady numerical simulation and investigated the effect of opening angle. Then, they compared the hemodynamic performance of St. Jude and CarboMedics heart valve prostheses and found out that the former one generates less disturbances due to its larger opening angle which is about 85°. Finally, with the help of a 3D numerical simulation and assumption of two symmetry planes, they reported that as the opening angle increases, the created wakes downstream of the valve gets smaller and move towards the center. However, larger opening angles are associated with higher maximum velocity and consequently higher shear rates. Another simplified 2D models were utilized to observe the flow domain through the BMHVs. For instance, Bluestein *et al.*<sup>9</sup> took into account the turbulence effects and conducted a transient simulation to capture the vortex formation in the flow passing a fully open St. Jude bileaflet valve. They reported that the vortex shedding leads to increase in the collision of molecular and cellular components of the hemostasis system and finally activates the platelets. Also, Bluestein *et al.*<sup>8</sup> investigated the effect of implantation angle of the heart valve prosthesis and expressed that formation of free emboli in the wakes of BMHV would be affected with implantation techniques. Also, Ge *et al.*<sup>22</sup> performed unsteady 3D laminar flow simulation with the assumption of flow symmetry and they doubted the validity of symmetry assumption by indicating that the flow has a highly 3D structure. In a work by Alemu and Bluestein,<sup>6</sup> they utilized a 3D model with the leaflets of the St. Jude valve and introduced a scalar stress value to quantify the blood damage in such flow fields. They measured total stress (shear, turbulent, deformation) and reported that trajectories of platelets that were recruited to the helical vortices experienced the highest stress accumulation values. In order to model the aortic root more and more accurately, Grigioni *et al.*<sup>23</sup> performed three-dimensional numeric simulation of flow through a bileaflet aortic valve in physiologic aortic root shaped model, in which no symmetry planes were exploited. In this work, fully open valve in the laminar flow at low regime was analyzed at the systolic phase. By comparing the numerical results with the experimental ones, they concluded that simulation with nonsymmetric realistic aortic root with three sinuses yields acceptable accu-

racy to predict the flow parameters downstream of the prosthetic valves.

As it was mentioned, there is a complex coupling in the case of hemodynamic performance of the BMHVs. In other words, the flow field inside the aorta would not be accurately analyzed unless the dynamics of the leaflets are taken into account. Therefore, the recent works have been concentrated on this multiphysics nature and tried to simulate the blood flow along with the heart valve dynamics simultaneously. It should be noted that in addition to thromboembolism, some other complications such as cavitation are associated with the valve motion during the opening and closure. For instance, in a recent study by Li,<sup>29</sup> closing dynamics of a new trileaflet and a bileaflet heart valve has been compared. They concluded that cavitation phenomenon which is caused by the excessively rapid velocity is more probable to occur in the BMHV due to its higher closing velocity. Effect of existence of the sinuses was investigated in two different types of blood vessels with and without sinus by Bang<sup>7</sup> where the leaflet angles during the cardiac cycle were reported too. In this fluid structure interaction simulation for curved BMHV, it was presented that the leaflet motion and the blood flow are being influenced by the removal of the sinuses and the closing phase last more in this case. Dumont *et al.*<sup>16–18</sup> proposed a FSI model in which they first utilized the dynamic mesh method of Fluent software package for the two-dimensional simulation of the mechanical heart valve. Afterward, they compared a BMHV hemodynamic performance and its induced shear stresses in two geometries representing mitral and aortic flow patterns. Other researches found out more complex 3D flow exists in the hinge area and considered the effect of hinge design i.e., leaflets ear and hinge recess. Finally, in later research, they compared two BMHVs, i.e. ATS open pivot and St. Jude, in a three-dimensional transient numerical simulation with an aortic flow waveform. In order to study the hinge area more and more precisely, some researches have been done with modeling the blood flow through only the hinge recess.<sup>39,40</sup> Finally, in a recent work by Kuan,<sup>27</sup> the most realistic model was presented for such studies. They used four different cases to consider the effects of aortic arch and sinuses of Valsalva. They reported different flow patterns in the hinge area under the influence of aortic arch. By comparing four hinge regions, they concluded that flow rate passing the valve is not changed considerably for each individual hinge.

Based on the brief review above and to the best of the authors' knowledge, there is a lack of information about On-X heart valve prosthesis which is relatively considered as the new generation ones. For example, in a review by Yoganathan *et al.*<sup>44</sup> a wide range of data for the hemodynamic performance of the different mechanical heart valves is presented while there is no

reported data for the On-X valves. Also, there have been several works in which the traditional mechanical heart valves such as St. Jude, ATS, CarboMedics, Jyros and Medtronic Hall have been compared to each other in terms of hemodynamic and design parameters.<sup>1–3,40</sup> However, in a set of experimental studies by Akutsu,<sup>4,5</sup> hemodynamic performance of three BMHVs, i.e., St. Jude, On-X and MIRA, has been compared with the help of dynamic particle image velocimetry (DPIV). They employed two prosthetic valve orientations and presented the flow field of both configurations for each valve. They reported that two newer designs, i.e. the On-X and the MIRA, offer a wider opening area in the fully open state. Also, they observed more deflected flow in the St. Jude valve comparing to the newer ones. In this experimental study, a simple jet-type flow for On-X valve was observed while for the MIRA valve with curved leaflets, more diffusive and consequently complex flow field was reported for the downstream of the aortic valve. In a more recent work by Akutsu, turbulence generated by the valves was also discussed. Turbulent flow is associated with more energy loss which may impose additional work on the heart and lead to hypertrophy in some cases. In addition, turbulent eddies increase the residence time of the blood cells in elevated high shear stress regions and therefore contribute to the platelet activation. In the mentioned work, they expressed that each valve is characterized by different turbulent strengths and scales. During the peak systole, the MIRA valve showed strong and broader turbulence. Finally, a recent research by Chambers *et al.*<sup>11</sup> presented a remarkable clinical performance of the On-X valves which indicates the need for investigation of its hemodynamic performance and its underlying reasons. Their results for the aortic valve replacement have been summarized in Table 1. These data were gathered from 3 European

centers in 12 years with a mean of 5.2 years after the replacement surgery.

Taking a look at this data, it is clear that this BMHV would yield low adverse clinical rates in long-term follow-up. Also a similar study by Palatianos<sup>37</sup> has been conducted and they concluded that in the case of aortic valve replacement, mean transvalvular pressure gradients are in the range of 8.3–4.3 mmHg. It is worth noting that they reported improved hemodynamic performance for these types of bileaflet valves.

In this work, this relatively new generation design BMHV, i.e., a 23-mm On-X Medical valve, is selected for FSI simulation. Figure 1 shows this valve from the above view. These valves is believed to show improved hemodynamic performance due to some innovations such as inlet flared orifice, larger opening angle and free-stasis pivot design.<sup>36</sup> The realistic model of the ascending aorta consisting sinuses of Valsalva is generated to model the blood flow through this valve precisely. Since the valve opening takes place in a very short time which induce an impact and its process go along with the maximum shearing force in the systolic phase, accurate modeling of this phenomenon is of importance. Therefore, the opening process is investigated in this study and blood flow characteristics along with the valve dynamic is analyzed inside the aorta.

## METHODS

In this section, the constructed *in silico* model which comprises both the fluid and structural domain is illustrated. In addition, the numerical approach and boundary conditions to resolve the governing equations are explained in details.

### Geometry

The selected valve model in this study is a simplified 23-mm On-X technology heart valve which is presented in Fig. 1. This valve should be mounted on the realistic aortic root. The On-X valve was selected for this work since it is currently one of the most promising BMHVs. Also, demo valve with 23-mm diameter is chosen for this simulation since it is the mostly used dimension in the surgeries.<sup>37</sup> In this matter, alongside the available information issued by the On-X Life Technology Inc.,<sup>36</sup> a point cloud from the demo valve was provided with the help of optic 3D scanning which is depicted in Fig. 2. Coordinate measuring machine (CMM) has been utilized as an optical measurement device with accuracy of up to 80  $\mu\text{m}$ .

The extracted point clouds along with the direct measurements are used to construct the final model *via*

**TABLE 1. Long-term follow-up data for patients with aortic valve replacement.**

Aortic valve replacements (N = 214)		
Age mean (year)	59.7	
Gender M/F	157/56	
Adverse event	Early (<30 days)	Late (>30 days)
Death number		
Sudden	0	5
Cardiac	2	4
Noncardiac	0	19
Valve related	0	2
Total	2	30

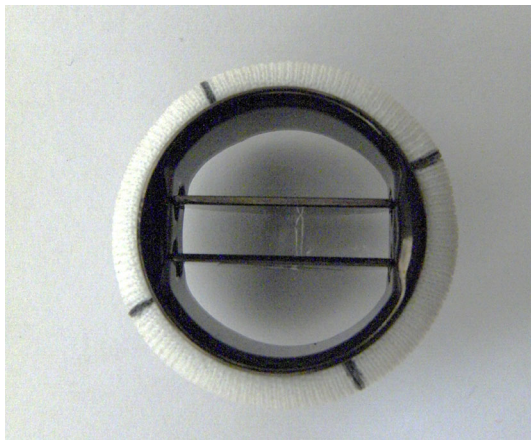


FIGURE 1. On-X mechanical heart valve from the top view in fully open position.

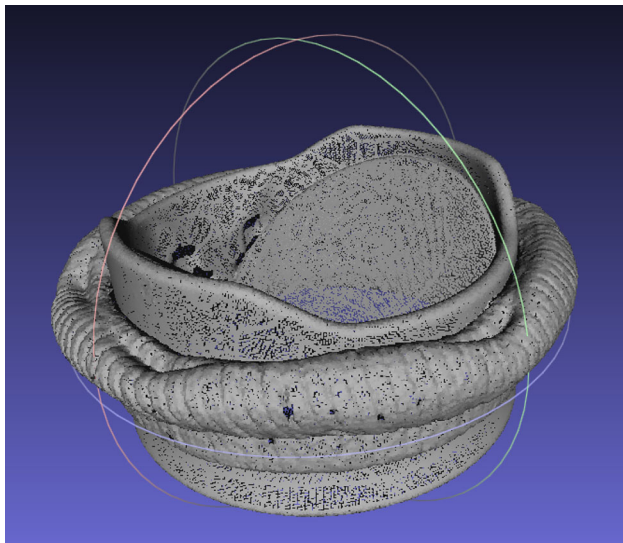


FIGURE 2. Point cloud of the BMHV achieved by CMM.

SolidWorks software. This would help smoothen the hinge recess and leaflet ear surfaces from the point clouds. These data were combined in order to generate a realistic 3D model of the BMHV by the SolidWorks software package. Spatial dimensions and components of the resulting valve model is presented in Fig. 3. It is clear that the sewing ring is omitted since it has no effect on the blood flow pattern inside the aortic valve.

For the valve leaflet with internal orifice area of  $3.41 \text{ cm}^2$ , the length is 13.5 mm, the thickness is 0.8 mm, and the free rotational angle is  $40^\circ$  to  $90^\circ$ .<sup>4,36</sup> With the On-X valve's patented "actuated pivot design", the leaflets are able to open full  $90^\circ$  before the closure phase.<sup>36</sup> Therefore, due to the symmetric geometry of the hinge and the leaflets, in the fully closed state of the valve, the traveling angle of the both leaflets is  $50^\circ$  which is shown in Fig. 4. Valve model is sectioned with two mid-planes parallel and perpendicular to the axis of rotation.

It is worth noting that the leaflet ear is located inside the non-symmetric hinge recess with the butterfly shape especially designed by On-X life technology Inc.<sup>36</sup> The small scale picture of this design and the modelled hinge area are illustrated in Fig. 5 with zooming in this region. As it is clear, the leaflet and its corresponding hinge are designed in such a way that an unswept area would be created in the corners of the hinge. This phenomenon make the flow pass the pivot with less potential flow stagnation and is a key to low thrombosis rate.<sup>36</sup>

As it is well known, there are some gaps in every BMHV designs which impose high shear stresses on blood cells passing through them. The gaps between the leaflets and the housing are aimed to provide the leaflet motion with minimum friction and consequently lead to lower transvalvular pressure gradient. However, elevated shear stresses are observed in the hinge recess, peripheral and bi-datum gaps which are shown in Fig. 6. For better understanding, one of the leaflets

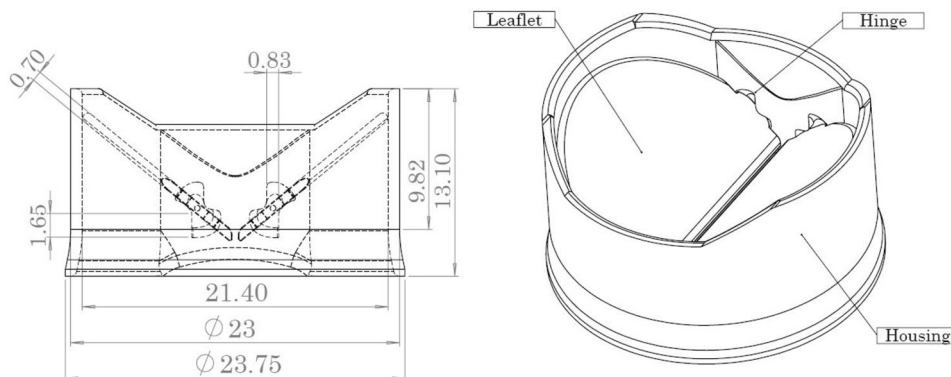
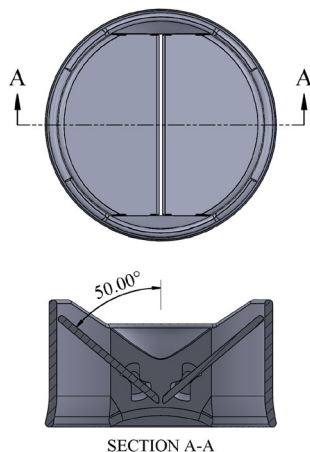


FIGURE 3. Spatial dimensions and components of On-X heart valve computer model in closed position.

is hidden in Fig. 5 and another one is shown with its ear placed in the hinge recess. The mentioned high shear stress may make the valve prone to clinical complications such as hemolysis and platelet activation. The b-datum gap width (Fig. 6a) i.e., the distance between the two leaflets in closed position is set to  $400\ \mu\text{m}$ . The peripheral gap (Fig. 6b) i.e. the distance between the leaflet tip and the housing is  $140\ \mu\text{m}$ . Also, as the clinical observations indicated,<sup>39</sup> the hinge gap width (Fig. 6c) i.e., the distance between the leaflet ear and hinge recess is adjusted to  $140\ \mu\text{m}$ . It should be mentioned that due to the complex geometry and high computational cost, these values may overestimate the real ones a bit. However, comparing to the nominal values of the valve this difference especially in the hinge is less than 5%.

The mentioned On-X valve is mounted on a realistic aorta model consisting of three sinuses of Valsalva and the downstream curved aortic arch (thoracic aorta). With respect to the aim of generating a generalized model, first of all a thoracic aorta point cloud have been extracted by the segmentation tools from computed tomography angiography (CTA) images of a



**FIGURE 4.** Leaflet traveling angle from fully closed to fully open position.

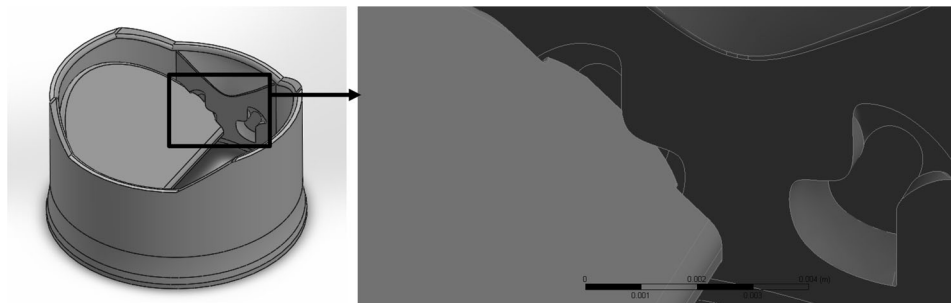


**FIGURE 5.** Hinge area and leaflet ear of the modelled On-X valve.

patient with implanted BMHV. The point cloud has been used to obtain the curvature centerline of the thoracic aorta. This data along with the dimensions available in the literature for an average person produced the final generalized model.<sup>19,31</sup> This geometry is constructed in SolidWorks software and the On-X valve is inserted into it. The resulting fluid domain is shown in Fig. 7.

It is worth noting that the leaflet surfaces are set as the fluid–solid interaction boundary at which the data transfer occurs. Calculated forces on these surfaces are exported from the flow solver, while the displacement is measured by the structural solver and is sent to the flow solver in order to update mesh at each coupling iteration. It should be noted that aorta is modelled as rigid wall since consideration of compliance effects imposes high computational cost on the solvers. Finally, it is worth noting that the fluid domain was subdivided to 3,610,146 tetrahedral elements to ensure there is sufficient number of nodes in the mentioned gaps to capture the main flow features. The mesh resolution is varied from  $20\ \mu\text{m}$  in the gaps to about  $800\ \mu\text{m}$  in areas distant from the walls. Figures 8a and 8b show the resulting computational domain in the vicinity of the mechanical valve and a cross section from the middle of the leaflets.

Also 283,789 tetrahedral and pyramid elements were used to discretize the structural domain. On the other hand, to resolve the small time scales and rapid velocity of the leaflets, the timestep is set to 0.5 ms.

It should be mentioned that different mesh sizes were used in order to conduct the grid independency study. In this way, transvalvular pressure gradient at peak systole as one of the most important parameters of the valve performance was compared for different number of cells. The number of cells is increasing from  $1.3 \times 10^6$  to  $8 \times 10^6$  and variation of the pressure gradient for different mesh sizes are presented in Fig. 9. Results indicate that  $3.6 \times 10^6$  cells are sufficient to predict the valve performance with less than 2% error.

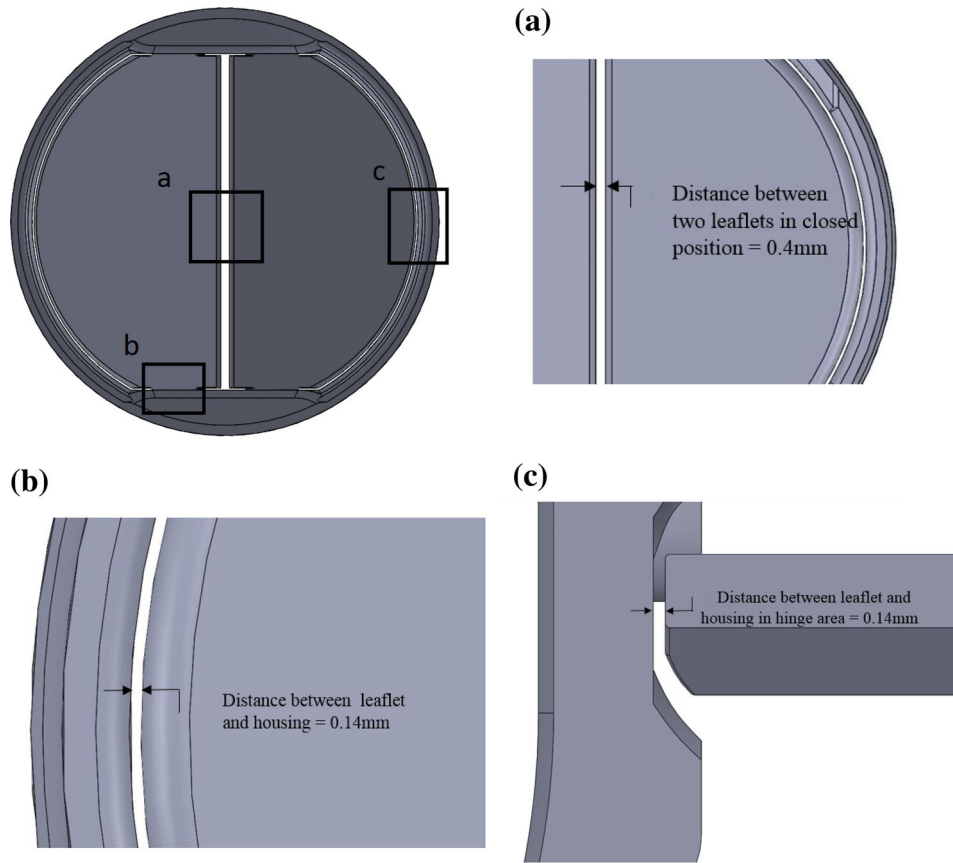


**FIGURE 6.** (a) b-datum gap between the leading edges of two leaflets (b) Peripheral gap between the leaflet tip and the housing (c) hinge gap between the hinge recess and the leaflet ear.



**FIGURE 7.** Fluid domain inside the ascending aorta with BMHV.

#### *Flow and Mechanical Solvers*

The blood flow is considered as incompressible flow in which the blood is modelled with Newtonian shear stress relations. Blood viscosity at a constant strain rate is affected by the tube diameter and hematocrit.

With respect to the volume fraction for a normal person and the aorta diameter, constant dynamic viscosity of 3.6 cP seems to be a logical assumption for this study.<sup>34</sup> Therefore the governing equations for this case is instantaneous Navier–Stokes (NS) equations which in tensor notation are given as follows:

$$\frac{\partial U_i}{\partial t} + \frac{\partial U_j U_i}{\partial x_j} = B_i - \frac{1}{\rho} \frac{\partial p}{\partial x_i} + \frac{1}{\rho} \frac{\partial \tau_{ij}}{\partial x_j}$$

where  $U$  is the instantaneous velocity vector,  $\rho$  is the density,  $p$  is the pressure,  $\mu$  is the dynamic viscosity of the fluid and  $B$  is the body force. The fluid density is considered  $1050 \text{ kg/m}^3$ .<sup>34</sup>

In order to evaluate the turbulence parameters in the flow field which is a key feature of the BMHVs as mentioned before, unsteady Reynolds-averaged Navier–Stokes (URANS) equations are utilized as follows:

$$\rho \frac{\partial u_i}{\partial t} + \rho \frac{\partial u_j u_i}{\partial x_j} = \rho B_i - \frac{1}{\rho} \frac{\partial p}{\partial x_i} + \frac{1}{\rho} \frac{\partial}{\partial x_j} \left( \mu \frac{\partial u_i}{\partial x_j} - \overline{u'_i u'_j} \right)$$

It should be noted that  $u$  represents the mean velocity vector and  $u'$  is the velocity fluctuation.

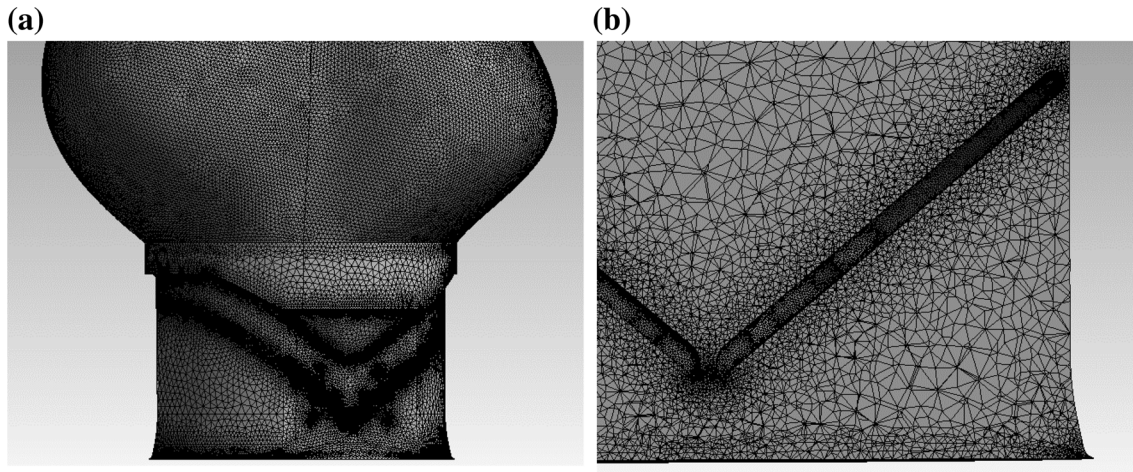


FIGURE 8. Computational mesh (a) near the valve region (b) cross section from middle of the leaflets.

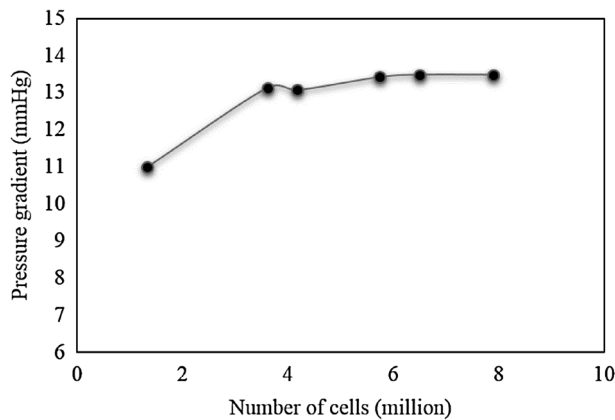


FIGURE 9. Grid independency study (transvalvular pressure gradient vs. mesh size).

Therefore, according to the URANS formulation, the total stress tensor can be defined in this way<sup>38</sup>:

$$\bar{\tau}_{ij} = \mu \left( \frac{\partial u_i}{\partial x_j} + \frac{\partial u_j}{\partial x_i} \right) - \rho \overline{u'_i u'_j}$$

With the help of Boussinesq approximation, i.e., turbulent viscosity hypothesis, Reynolds stresses can be expressed as a function of the mean flow field. Therefore, the final form of the total stress is defined as follows:

$$\bar{\tau}_{ij} = \mu \left( \frac{\partial u_i}{\partial x_j} + \frac{\partial u_j}{\partial x_i} \right) + \frac{2}{3} \rho k \delta_{ij} - \mu_t \left( \frac{\partial u_i}{\partial x_j} + \frac{\partial u_j}{\partial x_i} \right)$$

In order to obtain turbulent or eddy viscosity  $\mu_t$ , Realizable  $k-\epsilon$  model is chosen in which  $\epsilon$  is the turbulent dissipation rate and  $k$  is the turbulent kinetic energy. This model is capable of resolving complex flows with large strain rates such as recirculation and

strong pressure gradients which are exactly the case for the transient simulation of hemodynamic performance of BMHVs. With this approach, eddy or turbulent viscosity is obtained in this way:

$$\mu_t = \rho C_\mu \frac{k^2}{\epsilon}$$

where  $C_\mu$  is a variable dependent on the rate of deformation and spin tensors. Two transport equations are also solved for turbulent kinetic energy and dissipation rate.

A commercial solver Ansys Fluent 14.5 was chosen for simulation as the flow solver since it is capable of solving the flow domain in conjunction with transferring data to the mechanical solver. It sends acting forces on the leaflets to the Ansys Mechanical software which is responsible for solving the governing equations of solid domain i.e., valve leaflets. It should be noted that in the case of linear elastic solids, the corresponding stress tensor can be obtained by<sup>28</sup>:

$$\sigma_{ij} = \lambda \delta_{ij} e_{kk} + 2G e_{ij}$$

where

$$\lambda = \frac{Ev}{(1+v)(1-2v)} G = \frac{E}{2(1+v)}$$

$E$  is young modulus,  $G$  is the shear modulus,  $\nu$  is the Poisson ratio and  $e$  is the displacement gradient tensor. With the help of these formulations, the equations of motion for the solid part, i.e., the leaflets, are given by:

$$\rho a_j = \frac{\partial \sigma_{ij}}{\partial x_j} + B_j$$

The material properties of the pyrolytic carbon which has made the valve is considered to be incom-

pressible elastic linear solid with Young module of  $E = 25$  GPa and shear module of  $G = 9$  GPa. Also its density is considered  $2100 \text{ kg/m}^3$ .<sup>10,30</sup> In order to provide two-way coupling between both physics, the deflection and motion of the leaflets are transferred to the flow solver as the boundary displacement. Hence, Fluent will solve the governing equations in the updated flow field.

It should be noted that data transfer is managed by the Ansys System Coupling which connects the two solvers to each other in order to provide the problem with two-way fluid solid interaction. A transient simulation was defined with a total time period of 180 ms which corresponds to the time period of accelerating flow through the valve. These data points are corresponding to a cardiac output of 6.1 lit/min and heart rate of 75 beats/min. Time step of 0.5 ms was chosen for the simulation. The corresponding cardiac cycle and its simulated part which includes the valve opening is illustrated in Fig. 10. This physiologic flow rate is set as the inlet boundary condition for the fluid domain.<sup>27</sup> Also, the aortic pressure wave, which is depicted in Fig. 10 with red line, is assigned for the pressure outlet boundary condition, i.e., end of the ascending aorta. This pressure wave corresponded to the aortic blood pressure.<sup>34</sup>

It should be noted that the leaflets are in fully closed position at the initial moment.

## RESULTS AND DISCUSSION

In this section, the results of the fluid solid interaction simulation is presented in two parts. First, the streamlines and flow pattern are investigated precisely and flow induced stresses are calculated in order to analyze the thromboembolism potential in these valves. Afterward, the dynamic of the leaflets which is affected by the blood flow is analyzed. Results are tried to be presented for three main time points: mid-opening ( $t = 0.04$  s), open leaflets ( $t = 0.08$  s) and peak systole ( $t = 0.18$  s).

### *Blood Flow Pattern*

As it is well known in the medical approach, the blood flow through the valves should be as laminar as possible so as to minimize the energy loss and consequent pressure on heart. This favorable blood flow pattern will not be satisfied until the artificial organs provide an anatomical compatibility. Therefore, the geometry and blood flow pattern through BMHVs should be analyzed accurately in order to achieve the maximum possible physiologic conditions. First of all, the blood streamlines can give an initial insight into the

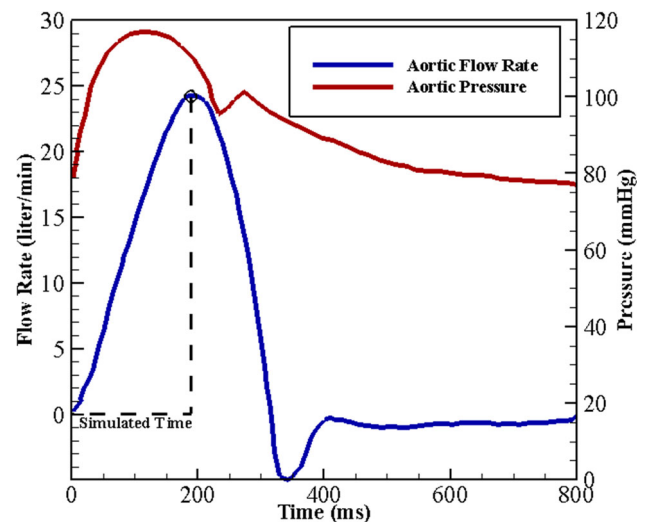


**FIGURE 10.** Physiologic flow and pressure waves of the ascending aorta.

flow pattern. Figure 11 depicted these paths colored by the velocity magnitude where the aorta and the valve are hidden to allow the streamlines seen easily from the side view when the leaflets are in fully open state.

As it can be inferred, the On-X valve can generate relatively uniform flow pattern with the help of its inlet flared orifice. Except the small area of recirculation in the sinus regions, the flow maintains its uniformity and seems to achieve the laminar state after damping the disturbances due to the leaflets. It is interesting to note that in the case of heart valve replacement, the sinuses lose their hemodynamic performance and some vortices are emerged in these regions which cannot take part in the valve closure. This is due to implantation of such valves in annulus and distance of leaflets from the sinuses. It should be noted that this flow pattern is in accord with Akutsu findings<sup>4,5</sup> in which they had reported that less diffusive flow was observed with the On-X valve and the flow turns into a jet-like pattern downstream of the valve. Another interesting parameter that is worth calculating is the velocity magnitude in the fluid domain which is influenced by the produced triple jet. The velocity contour in the mid-plane crossing the valve is given in Fig. 12a, again when the leaflets are fully open i.e., ( $t = 0.08$  s). Furthermore, it was claimed that triple-jet structure fades as the blood move inside the ascending aorta. This phenomenon is clear in Fig. 12b where three velocity contours at three different distances from the On-X valve have been presented. At the beginning of the aortic arch, it can be inferred that flow obtains its desired uniform shape and single-jet structure.

There is an interesting explanation for the opening angle of less than  $90^\circ$ . As it can be seen in the velocity



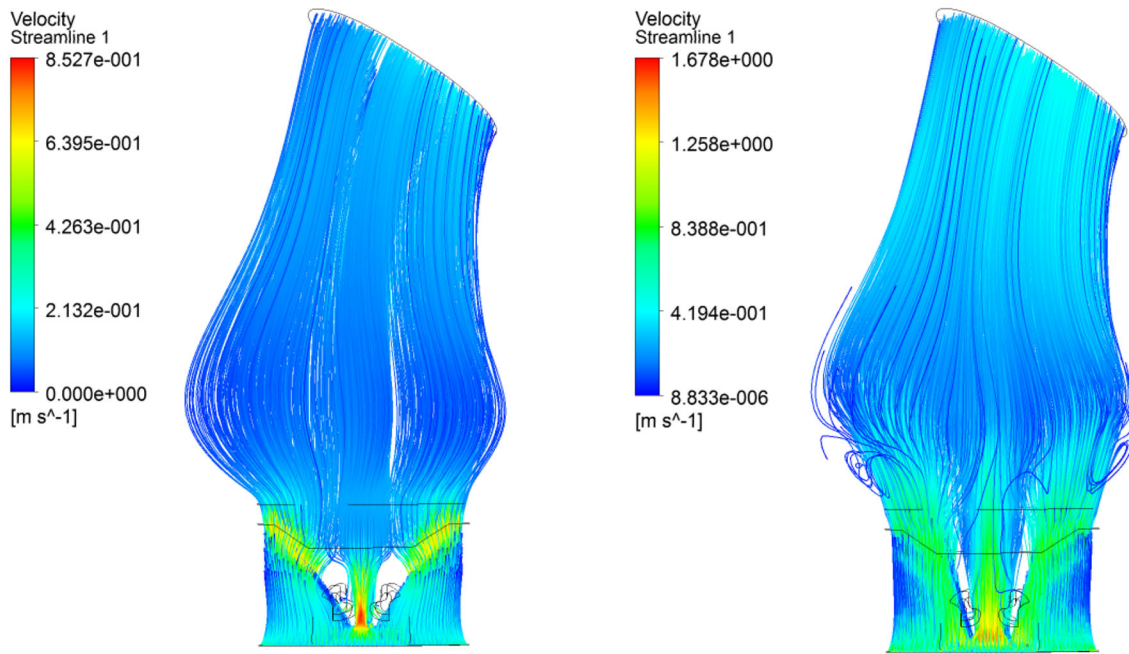


**FIGURE 11.** Blood streamlines in ascending aorta during opening process from the side view at mid-opening and fully open position of the leaflets.

contour, the three orifices make one diffuser-shaped and two nozzle-shaped areas for the blood flow. As a result, pressure increases a bit in the middle orifice and therefore this relative increase in pressure balances the flow induced impact and makes the leaflet flutter around approximately  $85^\circ$  position.

Moreover, it can be observed that the sinus region is filled with low-velocity blood which leads to vortex generation in the vicinity of this area. The triple-jet structure which is noticeable in Fig. 12a can also be visualized with the velocity profile near the valve. In order to verify the low diffusivity of the flow downstream of the valve, Fig. 13 shows the transverse velocity distribution in three different lines perpendicular to the leaflets orientation at three different distances from the valve. Although the lateral jets are stronger just downstream of the valve, they are kind of centralized and form a single flow stream in the aortic arch i.e., end of the ascending aorta. These profiles are presented for the open leaflets ( $t = 0.08$  s) time point.

Another important feature is the velocity magnitude and direction near the hinge recess. In other words, the microflow in this region as the most important factor for thrombus initiation and blood cell damage should be analyzed carefully. Figure 14 shows the velocity contours for two hinges on a plane parallel to the hinge floor inside the hinge recess. This plane is located at distance of  $300 \mu\text{m}$  from the hinge recess. Also, the velocity vectors are given in this plane so as to better understand the flow pattern in this small area.

It can be inferred that a lateral flow is created in this region which mostly contributes to the formation of vortices and stagnant points. However, due to the existence of two main streams in the hinge region, optimal pivot cleansing takes place which makes these valves distinct from the traditional ones.

The importance of laminar flow from the medical point of view was emphasized. Hence, it is useful to observe the procedure of formation of turbulent fluctuations and eddies during the accelerating systole which includes opening process of the valve leaflets. Figure 15 presented this event by depicting contours of the turbulent kinetic energy at four time points during this process.

It is clear that this energy loss and turbulence generation are started at vicinity of the leaflets which play role as the disturbance in the blood flow path. It is found out that the turbulence intensity is highest at the central jet. This event is due to the fact that blood impose the pressure on the down surface of the leaflets which cause them to rotate. Therefore, the most of the blood is encountered with two converging nozzles which increase the velocity and decrease the probability of flow separation and subsequent disturbances. On the other hand, it is worth analyzing the variations of turbulence intensity as the flow goes further from the valve. Figure 16 illustrates this trend with the help of turbulent kinetic energy contours at three separate planes which are located at different distances. As it can be seen, the turbulence intensity is decreased and

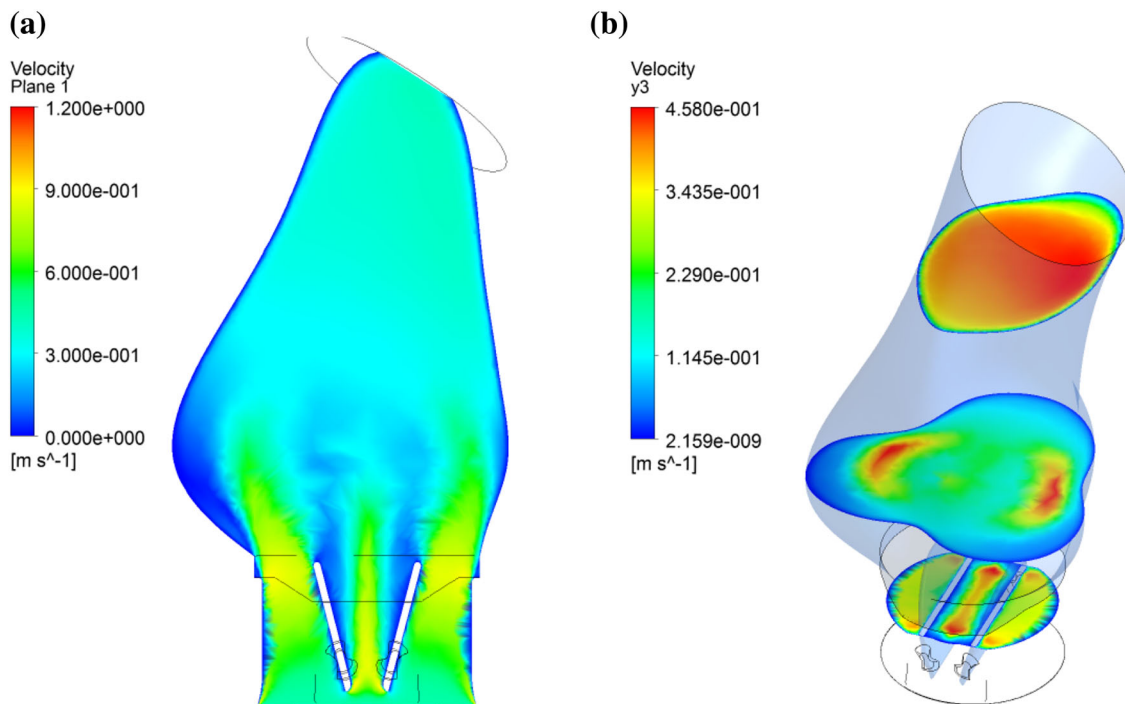


FIGURE 12. Velocity contours (a) at the mid-plane (b) at the three planes with different distances from the valve.

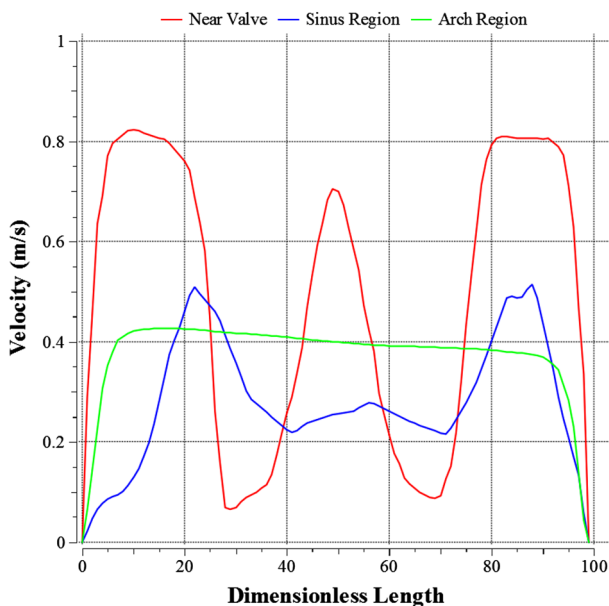


FIGURE 13. Variations of velocity profile with distance from the valve.

weakened. Hence, the desired laminar flow is achieved in the ascending aorta.

Finally, when the discussion is about the hemodynamic performance of the artificial heart valves, two parameters always have priority in evaluation and

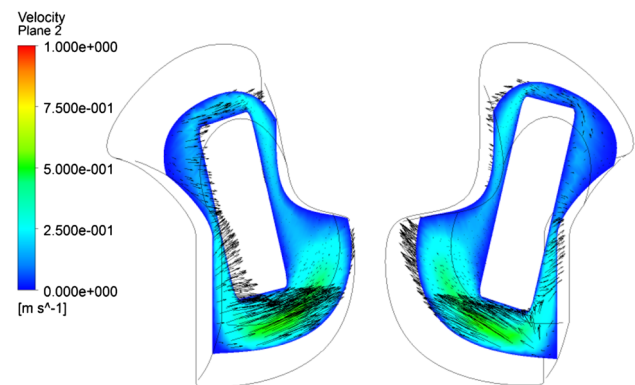
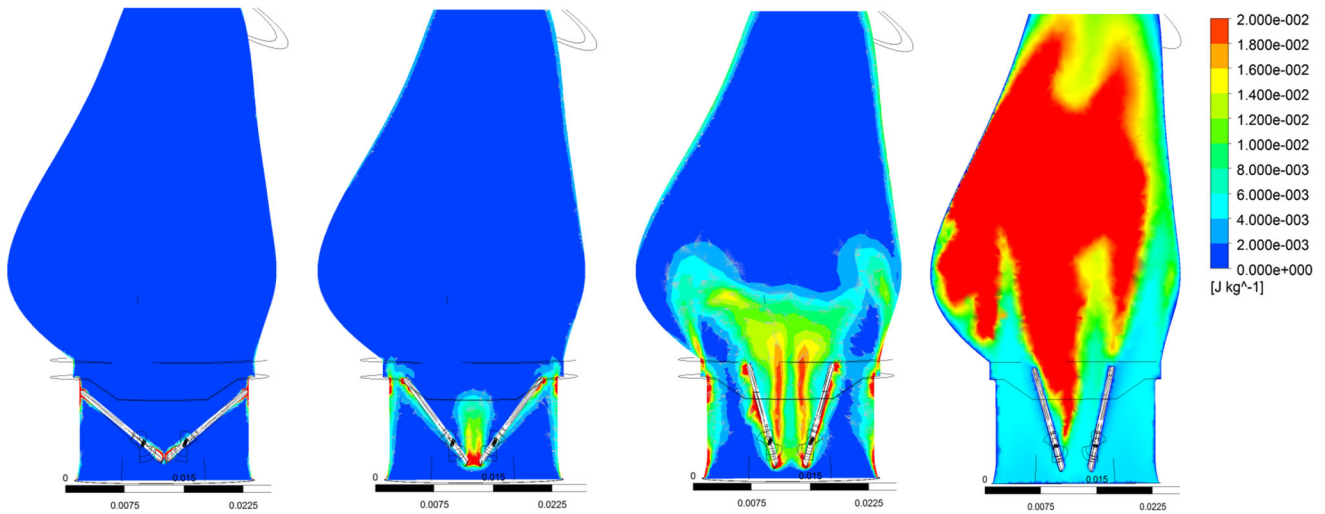
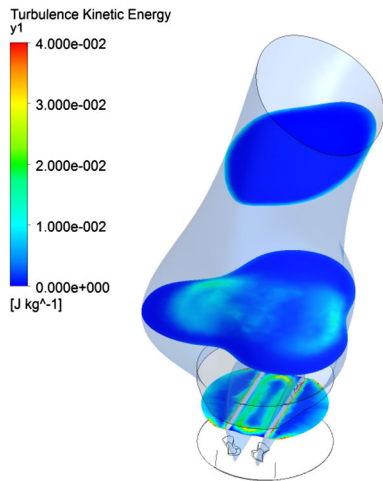


FIGURE 14. Velocity contours and vectors inside the hinge recess in a plane with distance of  $300\ \mu\text{m}$  from the hinge floor.

rating of the valve: pressure gradient and platelet activation. The former one is measured immediately after the replacement surgical procedure in order to ensure that heart would not be imposed to more external work and possible hypertrophy. The latter one also affects the patient in longtime due to the thromboembolism which is underlying reason of the long-term anticoagulant therapy. The transvalvular pressure gradients through the On-X heart valve in three time points are summarized in Table 2. With respect to the reported clinical values and available one in the literature<sup>37</sup> for the aortic peak, i.e.,  $12.3 \pm 6.2$  mmHg,



**FIGURE 15.** Evolution of turbulent flow (contours of turbulent kinetic energy at early systole, mid-opening, open leaflet and peak systole time points).



**FIGURE 16.** Contours of turbulent kinetic energy at three planes with different distances from the valve.

these are completely in the acceptable range and lower than the corresponding value for the traditional valves.

The platelet activation is also attributed to the shear stress on the fluid domain which is acting on the blood cell especially platelets. As it is well known in fluid mechanics, viscous stress tensor which is based on the mean velocity components is calculated by the following equation in tensor notation:

$$\tau_{ij} = 2\mu D_{ij}$$

$$D_{ij} = \frac{1}{2} \left( \frac{\partial u_i}{\partial x_j} + \frac{\partial u_j}{\partial x_i} \right)$$

While the turbulent stress tensor is given by:

$$(\tau_{ij})_t = 2\mu_t D_{ij}$$

The non-diagonal components of these stress tensors are called shearing stresses and should be measured in the whole domain. The maximum value of these shearing stresses is occurred in the hinge region due to the small area from which the flow is forced to pass. Therefore, the maximum of this parameter in three equally spaced planes parallel to the hinge floor wall at different distances are given in Table 3. It should be noted that from the molecular point of view, both stresses can be attributed to the collisions behind which albeit are different mechanisms. Therefore, it is believed that both stresses must be evaluated to ensure they do not meet the damage criteria.

These values indicate that the hinge recess is area of elevated high shear stresses that may lead to hemolysis and platelet activation. Another parameter which can exacerbate the blood cell situation is vortices due to their entrapping feature. Recirculating zones provide the blood cells with high exposure time and should be avoided in such valves especially in the leakage flow. In conclusion, recirculating zones should be distinguished in the domain since these regions are associated with thromboembolism. In this way, contours of the vorticity magnitude, i.e., curl of the velocity, are proper tool to investigate this event in the fluid domain. Figure 17 shows the formation of this parameter during the accelerating systole.

In order to obtain a better insight about the vorticity formation and its evolution through the domain, a criterion based on the work by Morbiducci<sup>33</sup> is defined for the vorticity magnitude. In this way, volume

**TABLE 2. Pressure gradient through the valve.**

Phase	Mid-opening	Fully open	Peak systole
Pressure gradient (mmHg)	4.96	7.05	13.41

**TABLE 3. Maximum shear stress at three critical planes.**

Shear stress component		Parallel planes to the pivot floor inside the hinge recess		
		$d = 0.15 \text{ mm}$	$d = 0.30 \text{ mm}$	$d = 0.45 \text{ mm}$
Maximum viscous shear stress (Pa)	$\tau_{xy}$	34.11	37.89	25.77
	$\tau_{xz}$	33.48	74.30	83.68
	$\tau_{yz}$	103.95	40.38	43.79
Maximum turbulent shear stress (Pa)	$\tau_{xy}$	16.35	24.70	25.52
	$\tau_{xz}$	17.38	19.62	14.57
	$\tau_{yz}$	35.01	19.31	21.63

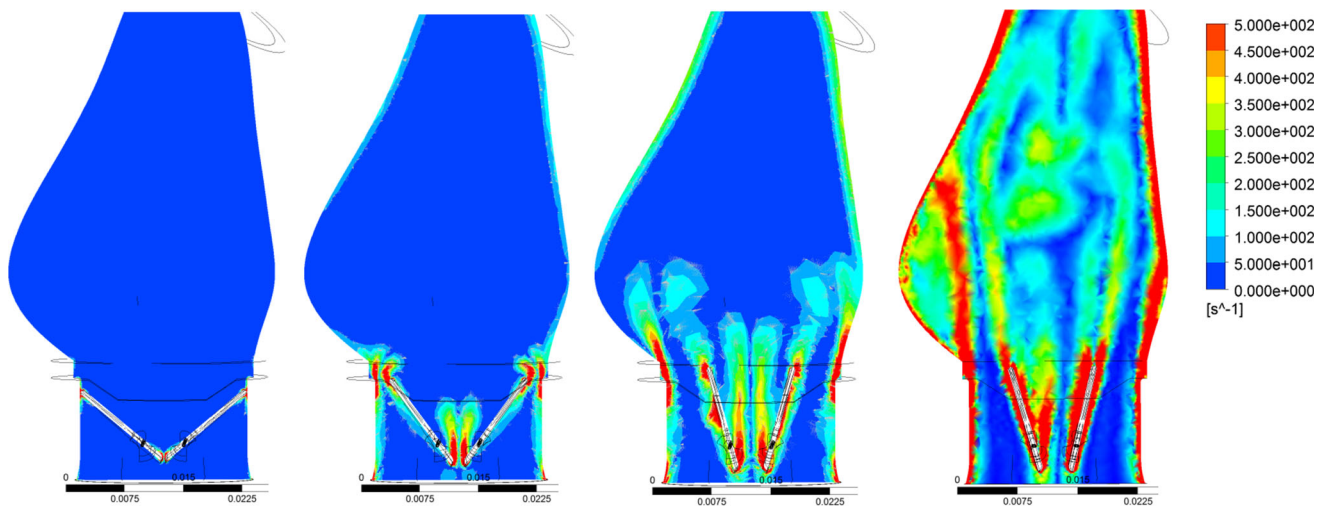


**FIGURE 17. Formation of vortices (contours of vorticity at early systole, mid-opening, open leaflet and peak systole time points).**

of the fluid with vorticity magnitude higher than  $800 \text{ s}^{-1}$ , which is correlated with the high risk of blood damage, is extracted from the fluid domain in different time points. As a sample, Fig. 18 shows the mentioned volume in the mid-opening and the fully open states. It is clear that vortical structures mainly evolve from the peripheral gap and they go downstream as the valve opens more and more. Due to the anatomy of the native aortic valve, this kind of vortices are absent in normal case; therefore, it can be concluded that coronary arteries blood flow may be influenced by these vortical structures which will be studied in the future work of this research group.

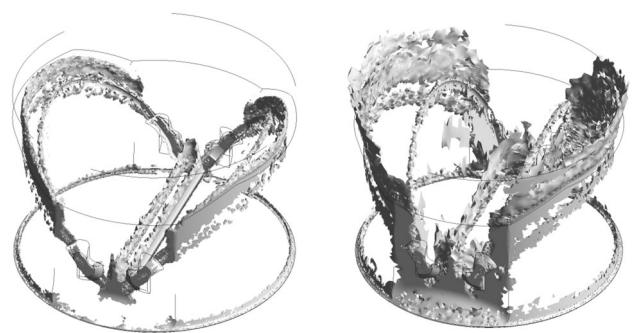


**FIGURE 18. Evolution of the high vorticity volume through the fluid domain.**

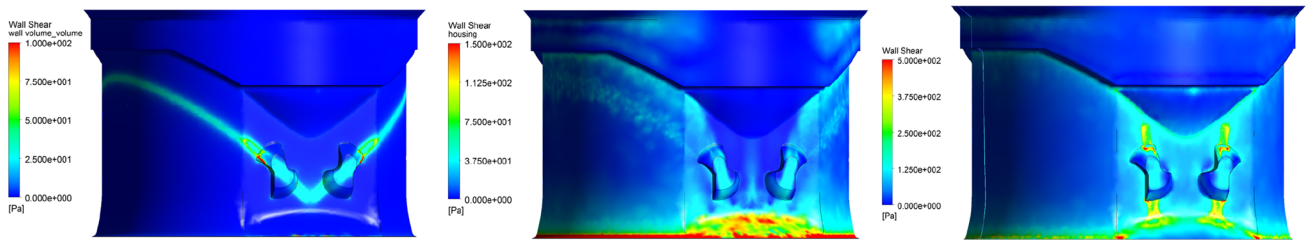


**FIGURE 19.** Distribution of the wall shear stress on the housing during the accelerating systole for three time points (mid-opening, open leaflets and peak systole).

**TABLE 4.** Leaflet maximum angular velocity at two phases of the motion.

Phase	Opening	Fluttering
Maximum angular velocity (rad/s)	11.49	3.71

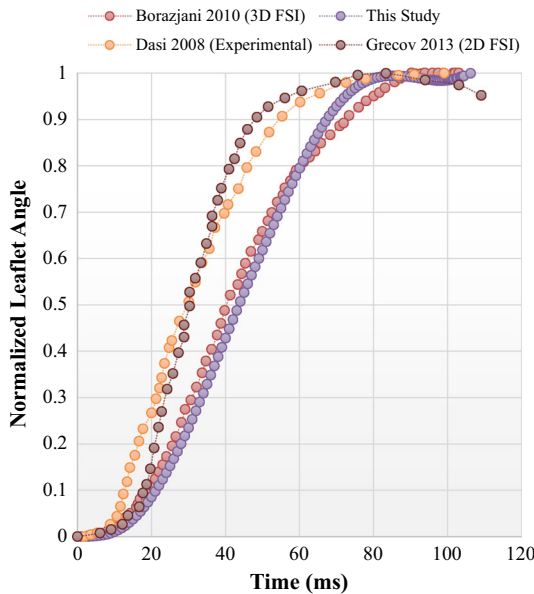


**FIGURE 20.** Normalized leaflet angle comparison.

Finally, wall shear stresses on the housing of the valve can also give another proper criterion to evaluate the potential of thrombus initiation in the vicinity of the valve. It is reported that for hemolysis this parameter must be about 400 Pa while in the case of platelet activation, even 10 Pa is enough to initiate this harmful process.<sup>27</sup> Distribution of the wall shear stress during the accelerating systole is illustrated in Fig. 19.

By taking a look at distribution of the wall shear stress in the housing, it can be inferred that although inlet flared orifice provide the flow with more uniform profile, it leads to increase in the wall shear stress due to the impact of the flow into the surface at this region.

### Valve Dynamics

The valve dynamics which is influenced by the flow-induced forces is of importance since it can contribute to some problems such as cavitation.<sup>32</sup> Therefore, the appropriate leaflet tip velocity should be achieved in order to avoid this kind of damages. Table 4 summarizes the maximum angular velocity of the leaflets during opening and fluttering phenomenon.

As it can be inferred, these velocities are lower than the reported values for the conventional valves and show similar behavior to that of the trileaflet valve.<sup>29</sup> This would stem from two reasons. First, lower traveling angle of the leaflets in this BMHV which is about 40° in this study. Second, comparing with the previous works, this study uses fully coupled solvers in addition to the exact modelling of the gaps in the geometry. Therefore, the resistant forces would increase in this case and consequently decrease the maximum angular velocity of the leaflets.

Furthermore, the leaflet normalized angle is observed through the opening process and is utilized as the validation factor. Figure 20 shows the normalized opening angle for this work along with the both numerical and experimental similar works which have been conducted recently.<sup>14,41,43</sup>

It can be inferred that all numerical simulations show a delay in opening prediction and this phenomenon could be attributed to the impulsive nature of the blood force. However, after the beginning, the employed method in this work is capable of predicting the experimental trend. In other words, by shifting the beginning moment, results are in agreement with the experimental ones. Moreover, the fluttering phenomenon is captured by this study which is reported in literature and its exact trend is hard to measure.<sup>35</sup>

### CONCLUSION

In this work, a relatively new generation design of the mechanical heart valves and its hemodynamic performance were studied. Due to some innovations

such as inlet flared orifice and new hinge design, this valve is believed to have resolved many of the problems associated with the traditional valves. Taking a careful look at the results, it is concluded that this type of BMHV is capable of producing a uniform and relatively laminar flow with decreased rate of vorticities. The low diffusive pattern of the blood flow passing the valve is in accord with the previous experimental works. The finding of this work which accounts for the effect of ascending aorta curve, is that large scale flow disturbances mostly fades before reaching the aortic arch. Also, results indicate that the formation of vortices and turbulent eddies is initiated at the vicinity of the valve leaflets. Furthermore, both turbulent and viscous shear stresses in the hinge recess and on the housing walls were evaluated. The value of these parameters proved that at the converging inlet and inside the hinges, blood cells especially platelets are in danger of elevated high shear stresses and subsequent thrombogenic complications. However, due to the existence of the recirculation zones just downstream of the valve and in the sinus regions, high residence time may initiate the thromboembolism. This phenomenon stems from the increase in particle collisions which mostly occurs in these areas. Finally, tip velocity of the leaflets during the opening phase implies that cavitation is not likely to happen.

#### ACKNOWLEDGMENT

The Authors of this paper would like to appreciate the helps and advices from all members of the Cardiovascular Hemodynamic Research Group which is a collaboration between the University of Tehran and Pars Hospital.

#### CONFLICT OF INTEREST

The authors declare that they have no conflict of interest.

#### STATEMENT OF HUMAN STUDIES

No human studies were carried out by the authors for this article.

#### STATEMENT OF ANIMAL STUDIES

No animal studies were carried out by the authors for this article.

#### REFERENCES

- <sup>1</sup>Akutsu, T., and D. Higuchi. Effect of the mechanical prosthetic mono- and bileaflet heart valve orientation on the flow field inside the simulated ventricle. *J. Artif. Organs* 3(2):126–135, 2000.
- <sup>2</sup>Akutsu, T., and D. Higuchi. Flow analysis of the bileaflet mechanical prosthetic heart valves using laser Doppler anemometer: effect of the valve designs and installed orientations to the flow inside the simulated left ventricle. *J. Artif. Organs* 4:113–125, 2001.
- <sup>3</sup>Akutsu, T., and T. Masuda. Three-dimensional flow analysis of a mechanical bileaflet mitral prosthesis. *J. Artif. Organs* 6(2):112–123, 2003.
- <sup>4</sup>Akutsu, T., and A. Matsumoto. Influence of three mechanical bileaflet prosthetic valve designs on the three-dimensional flow field inside a simulated aorta. *J. Artif. Organs* 13(4):207–217, 2010.
- <sup>5</sup>Akutsu, T., J. Saito, R. Imai, T. Suzuki, and X. D. Cao. Dynamic particle image velocimetry study of the aortic flow field of contemporary mechanical bileaflet prostheses. *J. Artif. Organs* 11(2):75–90, 2008.
- <sup>6</sup>Alemu, Y., and D. Bluestein. Flow-induced platelet activation and damage accumulation in a mechanical heart valve: numerical studies. *Artif. Organs* 31(9):677–688, 2007.
- <sup>7</sup>Bang, J. S., S. M. Yoo, and C. N. Kim. Characteristics of pulsatile blood flow through the curved bileaflet mechanical heart valve installed in two different types of blood vessels: velocity and pressure of blood flow. *ASAIO J.* 52(3):234–242, 2006.
- <sup>8</sup>Bluestein, D., Y. M. Li, and I. B. Krukenkamp. Free emboli formation in the wake of bi-leaflet mechanical heart valves and the effects of implantation techniques. *J. Biomech.* 35(12):1533–1540, 2002.
- <sup>9</sup>Bluestein, D., E. Rambod, and M. Gharib. Vortex shedding as a mechanism for free emboli formation in mechanical heart valves. *J. Biomech. Eng.* 122(2):125–134, 2000.
- <sup>10</sup>Böhlke, T., K. Jöchen, R. Piat, T.-A. Langhoff, I. Tsukrov, and B. Reznik. Elastic properties of pyrolytic carbon with axisymmetric textures. *Technische Mechanik* 30:343–353, 2010.
- <sup>11</sup>Chambers, J. B., J. L. Pomar, C. A. Mestres, and G. M. Palatianos. Clinical event rates with the On-X bileaflet mechanical heart valve: a multicenter experience with follow-up to 12 years. *J. Thorac. Cardiovasc. Surg.* 145(2):420–424, 2013.
- <sup>12</sup>Chandran, K. B. Role of computational simulations in heart valve dynamics and design of valvular prostheses. *Cardiovasc. Eng. Technol.* 1(1):18–38, 2010.
- <sup>13</sup>Cheng, R., Y. G. Lai, and K. B. Chandran. Three-dimensional fluid-structure interaction simulation of bileaflet mechanical heart valve flow dynamics. *Ann. Biomed. Eng.* 32(11):1471–1483, 2004.
- <sup>14</sup>Dasi, L. P., L. Ge, A. H. Simon, F. Sotiropoulos, and P. A. Yoganathan. Vorticity dynamics of a bileaflet mechanical heart valve in an axisymmetric aorta. *Phys. Fluids* 19(6):1–17, 2007.
- <sup>15</sup>Del Alamo, J. C., A. L. Marsden, and J. C. Lasheras. Recent advances in the application of computational mechanics to the diagnosis and treatment of cardiovascular disease. *Revista española de cardiología* 62(Vii):781–805, 2009.

- <sup>16</sup>Dumont, K., J. M. A. Stijnen, J. Vierendeels, F. N. van de Vosse, and P. R. Verdonck. Validation of a fluid-structure interaction model of a heart valve using the dynamic mesh method in fluent. *Comput. Methods Biomech. Biomed. Eng.* 7(3):139–146, 2004.
- <sup>17</sup>Dumont, K., J. Vierendeels, R. Kaminsky, G. J. Van Nooten, and D. Bluestein. Comparison of the hemodynamic and thrombogenic performance of two bileaflet mechanical heart valves using a CFD/FSI model. *J. Biomech. Eng.* 129(4):558, 2007.
- <sup>18</sup>Dumont, K., J. A. M. Vierendeels, P. Segers, G. J. Van Nooten, and P. R. Verdonck. Predicting ATS Open Pivot heart valve performance with computational fluid dynamics. *J. Heart Valve Dis.* 14(3):393–399, 2005.
- <sup>19</sup>Evangelista, A., F. A. Flachskampf, R. Erbel, F. Antonini-Canterin, C. Vlachopoulos, G. Rocchi, R. Sicari, P. Nihoyannopoulos, J. Zamorano, M. Pepi, O.-A. Breithardt, and E. Plonska-Gosciniak. Echocardiography in aortic diseases: EAE recommendations for clinical practice. *Eur. J. Echocardiogr.* 11(8):645–658, 2010.
- <sup>20</sup>Fortini, S., S. Espa, R. Toninato, L. Pacetti, M. F. Susin, and A. Cenedese. Analysis of the flow field downstream a bileaflet valve inside an aortic arch laboratory model, *16th Int Symp on Applications of Laser Techniques to Fluid Mechanics*, pp. 1–10, 2012.
- <sup>21</sup>Ge, L., L. P. Dasi, F. Sotiropoulos, and A. P. Yoganathan. Characterization of hemodynamic forces induced by mechanical heart valves: Reynolds vs. viscous stresses. *Ann. Biomed. Eng.* 36(2):276–297, 2007.
- <sup>22</sup>Ge, L., S. C. Jones, F. Sotiropoulos, T. M. Healy, and A. P. Yoganathan. Numerical simulation of flow in mechanical heart valves: grid resolution and the assumption of flow symmetry. *J. Biomech. Eng.* 125(5):709–718, 2003.
- <sup>23</sup>Grigioni, M., C. Daniele, C. Del Gaudio, U. Morbiducci, A. Balducci, G. D’Avenio, and V. Barbaro. Three-dimensional numeric simulation of flow through an aortic bileaflet valve in a realistic model of aortic root. *ASAIO J.* 51(3):176–183, 2005.
- <sup>24</sup>King, M. J., J. Corden, T. David, and J. Fisher. A three-dimensional, time-dependent analysis of flow through a bileaflet mechanical heart valve: comparison of experimental and numerical results. *J. Biomech.* 29(5):609–618, 1996.
- <sup>25</sup>King, M. J., T. David, and J. Fisher. An initial parametric study on fluid flow through bileaflet mechanical heart valves using computational fluid dynamics. *Proc. Inst. Mech. Eng. H* 203(1):1–14, 1994.
- <sup>26</sup>King, M. J., T. David, and J. Fisher. Three-dimensional study of the effect of two leaflet opening angles on the time-dependent flow through a bileaflet mechanical heart valve. *Med. Eng. Phys.* 19(3):235–241, 1997.
- <sup>27</sup>Kuan, Y. H., F. Kabinejadian, V.-T. Nguyen, B. Su, A. P. Yoganathan, and H. L. Leo. Comparison of hinge micro-flow fields of bileaflet mechanical heart valves implanted in different sinus shape and downstream geometry. *Comput. Methods Biomech. Biomed. Eng.* 18(16):1785–1796, 2015.
- <sup>28</sup>Lai, W. M., D. H. Rubin, D. Rubin, and E. Krempl. *Introduction to Continuum Mechanics*. Oxford: Butterworth-Heinemann, 2009.
- <sup>29</sup>Li, C.-P., and P.-C. Lu. Numerical comparison of the closing dynamics of a new trileaflet and a bileaflet mechanical aortic heart valve. *J. Artif. Organs* 15(4):364–374, 2012.
- <sup>30</sup>López-Honorato, E., P. J. Meadows, P. Xiao, G. Marsh, and T. J. Abram. Structure and mechanical properties of pyrolytic carbon produced by fluidized bed chemical vapor deposition. *Nucl. Eng. Des.* 238(11):3121–3128, 2008.
- <sup>31</sup>Mao, S. S., N. Ahmadi, B. Shah, D. Beckmann, A. Chen, L. Ngo, F. R. Flores, Y. L. Gao, and M. J. Budoff. Normal thoracic aorta diameter on cardiac computed tomography in healthy asymptomatic adults: impact of age and gender. *Acad. Radiol.* 15(7):827–834, 2008.
- <sup>32</sup>Mohammadi, H., and K. Mequanint. Prosthetic aortic heart valves: modeling and design. *Med. Eng. Phys.* 33(2):131–147, 2011.
- <sup>33</sup>Morbiducci, U., R. Ponzini, M. Nobili, D. Massai, F. M. Montevecchi, D. Bluestein, and A. Redaelli. Blood damage safety of prosthetic heart valves. Shear-induced platelet activation and local flow dynamics: a fluid-structure interaction approach. *J. Biomech.* 42(12):1952–1960, 2009.
- <sup>34</sup>Nichols, W., M. O’Rourke, and C. Vlachopoulos. McDonald’s blood flow in arteries. *Shock* 9(6):456, 1998.
- <sup>35</sup>Nobili, M., U. Morbiducci, R. Ponzini, C. Del Gaudio, A. Balducci, M. Grigioni, F. Maria Montevecchi, and A. Redaelli. Numerical simulation of the dynamics of a bileaflet prosthetic heart valve using a fluid–structure interaction approach. *J. Biomech.* 41(11):2539–2550, 2008.
- <sup>36</sup>“On-X Prosthetic Heart Valve Design and Features - On-X Life Technologies, Inc.” [Online]. Available: <http://www.onxli.com/medical-professionals/on-x-prosthetic-heart-valve-design-and-features/>. [Accessed: 22-Nov-2015].
- <sup>37</sup>Palatianos, G. M., A. M. Laczkovics, P. Simon, J. L. Pomar, D. E. Birnbaum, H. H. Greve, and A. Haverich. Multicentered European study on safety and effectiveness of the On-X prosthetic heart valve: intermediate follow-up. *An. Thorac. Surg.* 83(1):40–46, 2007.
- <sup>38</sup>Pope, S. B. *Turbulent Flows*. Cambridge: Cambridge University Press, 2000.
- <sup>39</sup>Simon, H. A., L. Ge, F. Sotiropoulos, and A. P. Yoganathan. Simulation of the three-dimensional hinge flow fields of a bileaflet mechanical heart valve under aortic conditions. *Ann. Biomed. Eng.* 38(3):841–853, 2010.
- <sup>40</sup>Simon, H. A., H.-L. Leo, J. Carberry, and A. P. Yoganathan. Comparison of the hinge flow fields of two bileaflet mechanical heart valves under aortic and mitral conditions. *Ann. Biomed. Eng.* 32(12):1607–1617, 2004.
- <sup>41</sup>Sotiropoulos, F., and I. Borazjani. A review of state-of-the-art numerical methods for simulating flow through mechanical heart valves. *Med. Biol. Eng. Comput.* 47(3):245–256, 2009.
- <sup>42</sup>Sotiropoulos, F., T. B. Le, and A. Gilmanov. Fluid mechanics of heart valves and their replacements. *Annu. Rev. Fluid Mech.* 48(1):150902153828003, 2016.
- <sup>43</sup>Yeh, H. H., D. Grecov, and S. Karri. Computational modelling of bileaflet mechanical valves using fluid-structure interaction approach. *J. Med. Biol. Eng.* 34(5):482, 2014.
- <sup>44</sup>Yoganathan, A. P., Z. He, and S. Casey Jones. Fluid Mechanics of Heart Valves. *Annu. Rev. Biomed. Eng.* 6(1):331–362, 2004.
- <sup>45</sup>Yun, B. M., J. Wu, H. A. Simon, S. Arjunon, F. Sotiropoulos, C. K. Aidun, and A. P. Yoganathan. A numerical investigation of blood damage in the hinge area of aortic bileaflet mechanical heart valves during the leakage phase. *Ann. Biomed. Eng.* 40(7):1468–1485, 2012.